Cited: Xu Lei. Electromagnetic brain imaging based on standardized resting-state networks. Paper presented at: 5th International Conference on Biomedical Engineering and Informatics (BMEI) (Chongqing, China). 2012 40-44.

Electromagnetic Brain Imaging Based on Standardized Resting-state Networks

Xu Lei
Key Laboratory of Cognition and Personality (Southwest University) and School of Psychology
Southwest University
Chongqing, China

***Abstract*—**We have recently proposed a electromagnetic brain imaging based on multiple fMRI spatial priors: NEtwork-based SOurce Imaging (NESOI) [Lei et al. "fMRI Functional Networks for EEG Source Imaging," *Human Brain Mapping*, vol. 32, pp. 1141-1160, 2011]. In our previous method, the spatial priors is extracted from the fMRI dataset on the same subject within the same paradigm. In this paper, we present a resting-state NEtwork-based SOurce Imaing (rsNESOI), which includes fMRI priors without extra fMRI scan. While simultaneous electroencephalogram (EEG) recording within fMRI scanner is available currently, rsNESOI is more convenient for EEG source reconstruction. The real data test suggests that rsNESOI is distinctly valuable in improvement of distributed source localization in contrast to the previous methods.

Keywords-EEG source imaging; fMRI; EEG; brain connectivity; resting-state networks

I. INTRODUCTION

Functional magnetic resonance imaging (fMRI), with its high spatial resolution in the order of millimeter, is helpful for electroencephalography (EEG) source localization [1]. A large number of previous studies have proposed possible approaches for including fMRI information as EEG imaging priors. In "fMRI-constrained dipole modelling" [2], the fMRI activation sites are used to initially seed dipoles within the active regions for further dipole fittings. These activation sites are regions that show positive blood oxygen level-dependent (BOLD) responses obtained from the Statistical Parametric Map (SPM) of fMRI. The "fMRI-constrained distributed inverse modelling" [3] used the SPM to weight the source space. The furter linear estimation provides an operator-independent method for combining information from fMRI and EEG. This method represents a significant advance over traditional dipole modeling [3].

Phillips et al. [4] proposed an empirical Bayes (EB) framework to combine fMRI active map in EEG source localization. In practice, the hierarchical statistical model in EB allows a variety of fMRI information to be introduced and each prior is controlled by hyperparameters determined by scalp EEG data. Based on this framework, we have recently proposed a electromagnetic brain imaging based on multiple fMRI spatial priors: NEtwork-based SOurce Imaging (NESOI) [5-6]. In NESOI, the spatial priors are the functional connectivity patterns extracted from the fMRI signal. Regardless of whether the EEG and fMRI measurements are simultaneous or conducted at different times, NESOI needs the suited EEG and fMRI recordings on the same subject within the same paradigm.

In this paper, using spatial patterns derived from resting-state fMRI, we standardized the functional connectivity networks for EEG source imaging. The newly proposed approach: resting-state NEtwork-based SOurce Imaing (rsNESOI), is free from fMRI scan but includes multiple fMRI priors as NESOI do. Comparing with other method with anatomical smoothness or sparseness constraints, rsNESOI can produce a solution that combines information of the high temporal resolution EEG and the high spatial resolution fMRI.

II. METHODS

A. Empirical Bayesian Model

An EB [4-5, 7-8] model used for EEG source location is,

$$Y = L\theta + \varepsilon \tag{1}$$

where $Y \in R^{n\times s}$ is the EEG recording with n channels and s samples. $\boldsymbol{L} \in R^{n\times d}$ is the lead-field matrix, and $\theta \in R^{d\times s}$ is the unknown source activity for d dipoles and $\theta \sim N(0, C)$. $N(0,\boldsymbol{C})$ denotes a multivariate Gaussian distribution with mean 0 and covariance C. The terms ε represent random fluctuations of channel and $\varepsilon \sim N(0, \alpha^{-1} I)$, where I_n is a n-by-n identity matrix. The spatial covariances of θ are mixtures of covariance components,

$$C = \sum_{i=1}^{10} \gamma_i V_i \ , \tag{2}$$

where $\gamma \equiv [\gamma_1, \gamma_2, \ldots, \gamma_{10}]^T$ is a vector of 10 non-negative hyperparameters that control the relative contribution of each covariance basis matrix, V_i. New we introduce how to construct the covariance basis matrix.

This research was supported by the National Nature Science Foundation of China (31200857), Fundamental Research Funds for the Central Universities (SWU1209319), National Key Discipline of Basic Psychology at Southwest University (NSKD11047) and Humanity and Social Science Youth foundation of Ministry of Education of China (12YJC190015).

B. *Extraction of Resting-state Networks*

The functional connectivity networks were extracted from a resting-state fMRI dataset. Forty-two healthy participants (20 females, age 18-27) provided written, consent at Southwest University. The experiment contained a 5 minute scanning and subjects were instructed to relax and close their eyes. Imaging were acquired with a 3T Siemens Trio scanner by echo planar imaging sequence: repeat time (TR) = 1.5 s, echo time (TE) = 29 ms, flip angle = 90 °, acquisition matrix = 64^2, in-plane resolution 3.0^2 mm^2, FOV = 192^2 mm^2, axial slices = 25, thickness/gap = 5/0.5 mm. All the data were mainly preprocessed with the spm8 (http://www.fil.ion.ucl.ac.uk/spm/), which implements slice acquisition timing, normalization and smoothing. Three subjects were excluded due to major head movements. The preprocessed functional image were subjected to a group spatial independent component analysis (ICA) as implemented in GIFT (http://icatb.sourceforge.net/).

TABLE I. STANDERDIZED RESTING-STATE NETWORKS

No.	*Resting-state network*	*Anatomic-Automatic-Labeling*
1	Medial visual areas	43 44 45 46 47 48
2	Occipital visual areas	49 50 51 52 53 54
3	Lateral visual areas	55 56 89 90
4	Default mode network	23 24 25 26 35 36 65 66 67 68
5	Sensorimotor	1 2 19 20 57 58 69 70
6	Auditory	17 18 63 64 81 82
7	Executive control	7 8 9 10 31 32
8	Left-lateralized frontoparietal	11 13 15 61 63 83 85
9	Right-lateralized frontoparietal	12 14 16 62 64 84 86

Spatial patterns of resting-state fMRI were displayed and explained based on the result of Smith et al. [9]. The intensity values in each pattern are scaled to z scores and voxels with absolute z scores >3 were considered to be activated. Nine resting-state networks were extract because their similar spatial distribution with [9]. Spatial patterns were further standardized with the Anatomic-Automatic-Labeling (AAL) atlas template [10]. The standardized resting-state networks involved nine spatially consistent patterns across different subjects, their AAL areas were listed in Table I. The first three resting-state network are correspond to medial, occipital pole, and lateral visual areas. Default mode network was a large structure, involes ten AAL areas. Sensorimotor, auditory and executive control networks were usually utilized by the brain in some special action. Left- and right-lateralized frontoparietal were the only maps to be strongly lateralized. They covered several frontoparietal areas.

Previous study has tested that resting-state networks were closely matched with the functional networks used by the active brain undergoing a comprehensive set of task types [9]. In literature [9], Smith et al. concluded that these resting-state network is continuously and dynamically "active" to constitute the full repertoire of functional networks utilized by the brain in action. We assumed these pattern may facilitate EEG source estimation. As shown in Figure 1, these networks have fixed AAL areas and employing them as standard priors will free from extra fMRI scan.

C. *Construction Spatial Priors*

In the source space, there are some areas not occupied by the above nine resting-state networks and they construct the tenth networks, i.e. the rest resting-state network. A simple way to construct a covariance component Vi from the ith network is to assign the diagonal terms with one if its correspond areas is involed in ith network, and the other terms with zero. The educed rsNESOI utilizes the patterns to improve localization accuracy. Based on the priors, rsNESOI is solved by restricted maximum likelihood (ReML) [7].

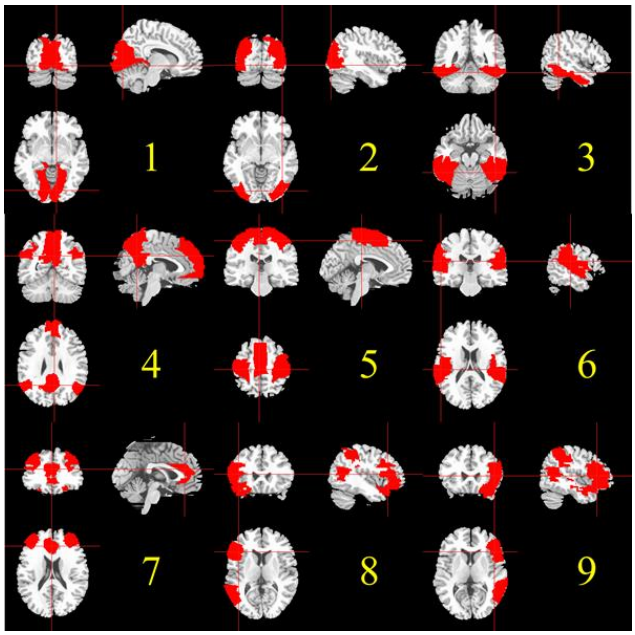

Figure 1. The standerdized nine resting-state networks. Sagittal, coronal, and axial views of the spatial map are listed for each network.

D. *Procedure of rsNESOI*

The raw EEG data is processed for artifact-rejection and event-related potentials (ERPs) are extracted. The standard resting-state networks are projected onto the surface mesh, leading to the definition of the covariance components of EEG source imaging. The intensity of the neural electric sources of ERPs are iteratively estimated by Restricted maximum likelihood (ReML) algorithm. The complete procedure of rsNESOI is illustrated in Figure 2. A face specific ERP "N170" was used to provide some provisional validation of the rsNESOI through model comparison.

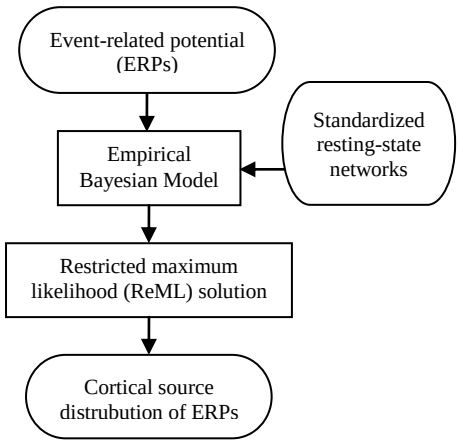

Figure 2. Schematic representation of the resting-state network-based source imaging (rsNESOI).

III. RESULT

The dataset contains signal from the same subject within the same paradigm, allowing extracting differential ERPs between faces and scrambled faces (http://www.fil.ion.ucl.ac.uk/spm/data/mmfaces/). The EEG data was first preprocessed with re-referencing to the average, and the artifact trials were rejected. Artifacts were defined as time-points that exceeded an absolute threshold of 120 μV (these were found primarily in the VEOG). Eighty of the 344 trials were rejected due to artifacts in total. The differential ERPs between faces and scrambled faces were utilized for further EEG source imaging. Resulting ERPs were then baseline-corrected from -200 ms to 0 ms and its spatial distribution are shown in Figure 3. The ERP obviously exhibited an activity peak around 170 ms following stimulus onset, in accord with a face specific "N170" [11].

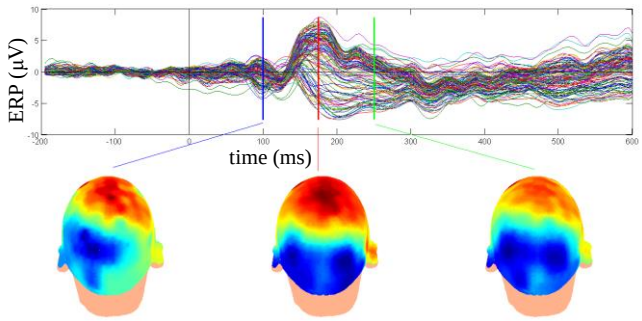

Figure 3. The differential ERPs between faces and scrambled faces. Spatial distributions are shown at 100 ms, 175 ms and 250 ms after stimulus onset, and a peak wave can be found around 170 ms.

After extracting differential ERPs between faces and scrambled faces, rsNESOI was employed for source reconstruction. The results are shown in Figure 4. These images showed 512 dipoles, with the greatest activity occurring at 170 ms.

Meanwhile, we employed classical Minimum Norm Estimation (MNE) [12-13] and multiple sparse priors (MSP) [7] for model comparison. In the MNE, covariance component is simply an identity matrix.

$$V_1^{MNE} = I_n, \tag{3}$$

where I_n is the n-by-n identity matrix, indicates that the sources are uncorrelated and widely distributed with equal amplitude. On the basis of uniform sampling of solution space, Friston et al. [7] proposed MSP model to describe activities in 128 patterns with the components as,

$$V_i^{MSP} = q_i q_i^T \ , \tag{4}$$

where q_i has diagonal terms with one if its correspond areas is sampled with MSP and the other terms with zero.

In Figure 4, the reconstructed profile of MNE was substantially more superficial and dispersed. The activations revealed by MNE were mainly located in the bilateral striate and extrastriate visual cortex of Brodmann's area (BA) 17 and 18. Meanwhile, with 128 components per hemisphere (i.e., 384=3×128 components in all), MSP uniformly sampled the source space and revealed activity in bilateral middle and superior temporal gyrus (BA 21/38). The results of the MSP inversion are partially consistent with MNM, but the deep and frontal sources (BA 21/38) were revealed more clearly. MSP also reconstructed activities in bilateral middle and superior temporal gyrus (BA 21/38).

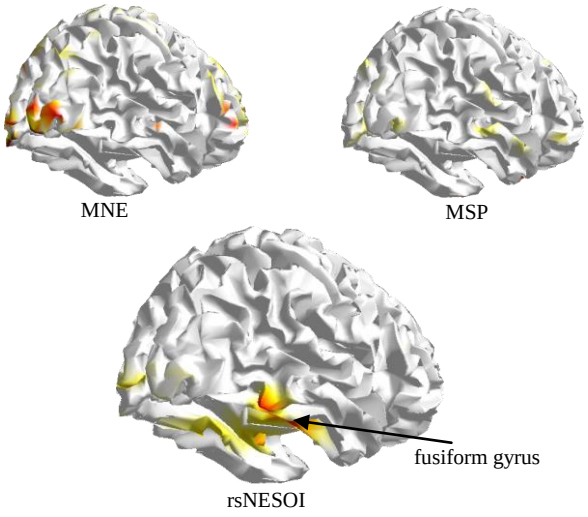

Figure 4. Maximum intensity projections of the spatial activities of face perception obtained by MNM, MSP and rsNESOI.

With the priors of standardized resting-state networks, five clusters were reconstructed by rsNESOI. The most active source is pointed with an arrow Figure 4. Both lateral with Talairach coordinates (52 -58.1 -21 mm) and medial with

Talairach coordinates (32 -40 -18 mm) mid-fusiform were reconstructed in the right temporal lobe. A weak source was also found in the left fusiform gyrus (-34 -41 -17 mm). This area might be the generator of the negative left occipital potentials in the EEG topography in Figure 3. In summary, compared with the other four methods, rsNESOI indicated much stronger activations in the right fusiform gyrus and medial frontal area, and a weak source in left fusiform. These results are in accordance with both the scalp potential map and previous studies of brain activations measured in a group of eighteen subjects using fMRI SPM [7].

We should emphasize that only EEG signal was used in this study. The spatial priors were derived from another study of resting-state fMRI. As previous study has proved that resting-state networks were closely matched with the functional networks used by the active brain undergoing a comprehensive set of task types [9], with automatic selection the reverence resting-state, the accuracy of EEG source imaging was improved greatly.

IV. Discussions

In this paper, we have described a new approach for EEG source imaging, rsNESOI, to employ resting-state networks to the distributed source reconstruction problem without extra fMRI scan. Our key contribution is the employment of standardized resting-state networks in the EB model. Previous study has shown that resting-state networks constitute the full repertoire of functional networks utilized by the brain in action. Our real data test has demonstrated the validity and effectiveness of the method. The results suggest that rsNESOI is distinctly valuable in improvement of distributed source localization. As resting-state networks established from fMRI are always disturbed by low temporal resolution, rsNESOI can be applied to provide more temporal details of these networks.

A large number of algorithms based on neuronal-anatomical priors have been previously reported. These approaches have used spatially based priors derived from MRI spatial information [4], an assumption that neighboring nodes exhibit similar neuronal activity [7], activation priors [1] derived from fMRI signal. In our previous NESOI approach [5-6], temporally coherent networks in the brain, including networks found during a resting state and those active during cognitive tasks, were utilized in EEG source imaging. In the current study, we extracted the major covarying networks in the resting brain, as imaged with fMRI in 42 subjects at rest. This result show these standardized resting-state networks can facilitate EEG source estimation.

In rsNESOI, we employ an empirical Bayes model to found the electrophysiology related standardized resting-state networks. Multiple networks spatial patterns are input as priors for analyzing EEG topography. This strategy enables sparse mappings of the common neuronal substrate between EEG and standardized resting-state networks [14]. With ReML algorithm, the reverence spatial patterns are automatically selected and localization accuracy is distinctly improved [14]. Similar strategy is popularly utilized in EEG-fMRI fusion, no matter data-driven or model-driven methods [15].

One application of rsNESOI is analyzing event-related potentials (ERPs), which is illustrated in our real-data test in this study. As our standardized resting-state networks established from fMRI may constitute the full repertoire of functional networks utilized by the brain in action. Those spatial pattern is useful to accurately localize the ERP.

Another potential application of rsNESOI is analyzing resting-state EEG, especially localization the spectral powers of varied bands. The rhythms in different bands has been reported interact with each other in several contexts, suggesting the possibility that different frequency oscillations might carry different dimensions of the integration process. The amplitudes of high-frequency oscillations were dynamically modulated by the phase of co-occurring theta-band oscillations in decision-making [16]. It was concluded that low frequency is robust for long-distance synchrony, while high frequency tend to be more stable for local patches of synchrony [17]. Further extend of rsNESOI will consider the cortical rhythms of EEG default mode network.

References

[1] A. M. Dale, A. K. Liu, B. R. Fischl, R. L. Buckner, J. W. Belliveau, et al., "Dynamic statistical parametric mapping: combining fMRI and MEG for high-resolution imaging of cortical activity," Neuron, 2000 vol. 26, pp. 55-67.

[2] K. Whittingstall, G. Stroink, and M. Schmidt, "Evaluating the spatial relationship of event-related potential and functional MRI sources in the primary visual cortex," Hum Brain Mapp, 2007 vol. 28, pp. 134-42.

[3] A. K. Liu, J. W. Belliveau, and A. M. Dale, "Spatiotemporal imaging of human brain activity using functional MRI constrained magnetoencephalography data: Monte Carlo simulations," Proc Natl Acad Sci U S A, 1998 vol. 95, pp. 8945-50.

[4] C. Phillips, M. D. Rugg, and K. J. Fristont, "Systematic regularization of linear inverse solutions of the EEG source localization problem," Neuroimage, 2002 vol. 17, pp. 287-301.

[5] X. Lei, P. Xu, C. Luo, J. Zhao, D. Zhou, et al., "fMRI Functional Networks for EEG Source Imaging," Human Brain Mapping, 2011 vol. 32, pp. 1141-1160.

[6] X. Lei, J. Hu, and D. Yao, "Incorporating fMRI Functional Networks in EEG Source Imaging: A Bayesian Model Comparison Approach," Brain topography, 2012 vol. 25, pp. 27-38.

[7] K. Friston, L. Harrison, J. Daunizeau, S. Kiebel, C. Phillips, et al., "Multiple sparse priors for the M/EEG inverse problem," Neuroimage, 2008 vol. 39, pp. 1104-20.

[8] X. Lei, P. Yang, and D. Yao, "An empirical bayesian framework for brain-computer interfaces," IEEE Trans Neural Syst Rehabil Eng, 2009 vol. 17, pp. 521-9.

[9] S. M. Smith, P. T. Fox, K. L. Miller, D. C. Glahn, P. M. Fox, et al., "Correspondence of the brain's functional architecture during activation and rest," Proceedings of the National Academy of Sciences, 2009 vol. 106, pp. 13040-13045.

[10] N. Tzourio-Mazoyer, B. Landeau, D. Papathanassiou, F. Crivello, O. Etard, et al., "Automated anatomical labeling of activations in SPM using a macroscopic anatomical parcellation of the MNI MRI single-subject brain," Neuroimage, 2002 vol. 15, pp. 273-89.

[11] R. N. Henson, Y. Goshen-Gottstein, T. Ganel, L. J. Otten, A. Quayle, et al., "Electrophysiological and haemodynamic correlates of face perception, recognition and priming," Cerebral Cortex, 2003 vol. 13, pp. 793-805.

[12] C. Phillips, J. Mattout, M. D. Rugg, P. Maquet, and K. J. Friston, "An empirical Bayesian solution to the source reconstruction problem in EEG," Neuroimage, 2005 vol. 24, pp. 997-1011.

[13] X. Lei, P. Xu, A. Chen, and D. Yao, "Gaussian source model based iterative algorithm for EEG source imaging," Comput Biol Med, 2009 vol. 39, pp. 978-88.

[14] X. Lei, C. Qiu, P. Xu, and D. Yao, "A parallel framework for simultaneous EEG/fMRI analysis: Methodology and simulation," Neuroimage, 2010 vol. 52, pp. 1123-34.

[15] X. Lei, P. Valdes Sosa, and D. Yao, "EEG/fMRI fusion based on independent component analysis: integration of data-driven and model-driven methods," Journal of Integrative Neuroscience, 2012 vol. 11, pp. 1-25.

[16] A. B. Tort, M. A. Kramer, C. Thorn, D. J. Gibson, Y. Kubota, et al., "Dynamic cross-frequency couplings of local field potential oscillations in rat striatum and hippocampus during performance of a T-maze task," Proc Natl Acad Sci U S A, 2008 vol. 105, pp. 20517-22.

[17] B. L. Foster and J. Parvizi, "Resting oscillations and cross-frequency coupling in the human posteromedial cortex," Neuroimage, 2012